EPJ Web of Conferences **90**, 08003 (2015)
DOI: 10.1051/epjconf/ 20159008003

Universal geometrical scaling of the elliptic flow

C. Andrés[1], J. Dias de Deus[2], A. Moscoso[1], and C. Pajares[1,a] Carlos A. Salgado[1]

[1] *Departamento de Física de Partículas and IGFAE, Universidade de Santiago de Compostela, 15782, Santiago de Compostela, Spain*
[2] *CENTRA, Departamento de Física, Instituto Superior Técnico, Av. Rovisco Pais, 1049-001, Lisboa, Portugal*

Abstract. The presence of scaling variables in experimental observables provide very valuable indications of the dynamics underlying a given physical process. In the last years, the search for geometric scaling, that is the presence of a scaling variable which encodes all geometrical information of the collision as well as other external quantities as the total energy, has been very active. This is motivated, in part, for being one of the genuine predictions of the Color Glass Condensate formalism for saturation of partonic densities. Here we extend these previous findings to the case of experimental data on elliptic flow. We find an excellent scaling for all centralities and energies, from RHIC to LHC, with a simple generalization of the scaling previously found for other observables and systems. Interestingly, the case of the photons, difficult to reconcile in most formalisms, nicely fit the scaling curve. We discuss on the possible interpretations of this finding in terms of initial or final state effects.

1 Introduction

The discovery of a sizable elliptic flow in AA collisions, first observed at RHIC [1, 2] and later at LHC [3], turned up as an experimental major breakthrough. The observed anisotropic flow can exclusively be understood if the measured particles in the final state depend not only on the physical conditions realized locally at their production point, but also on the global geometry of the event. This non-local information can solely emerge as a collective effect, requiring strong interaction among the relevant degrees of freedom, i.e. quarks and gluons. The study of higher harmonics has also shown very interesting features, including the ridge structure seen in AA collisions [4–7], pPb collisions [8, 9] and also in high multiplicity pp collisions [10]. The conventional understanding of the ridge is simply related to flow harmonics in a hydrodynamic scenario, where the description of the pPb ridge and, specially, the high multiplicity pp ridge is a challenge. The question is whether an initial state effect could determine the ridge structure. Or, in other words, if the elliptic flow is an initial state effect or, on the contrary, a final state effect amenable to a hydrodynamic description [11–21]. Along these lines, we study the possibility that an initial state property, as geometrical scaling due to gluon saturation, was preserved in a similar scaling in the elliptic flow. Similar questions related to how hydrodynamic descriptions could fit scaling laws observed in v_2 have already been raised [22].

[a] e-mail: pajares@fpaxp1.usc.es

2 Geometrical scaling in multiplicity distributions

Our work is based on a previous result, the geometrical scaling of multiplicity distributions in pp, pA and AA collisions [23–27], namely,

$$\frac{1}{N_A}\frac{dN_{ch}}{dp_T^2} = \frac{1}{Q_0^2}F(\tau), \tag{1}$$

where τ is known as the scaling variable and is given by

$$\tau = \frac{p_T^2}{\left(Q_s^A\right)^2}, \tag{2}$$

with $\left(Q_s^A\right)^2$ the saturation scale, and $Q_0^2 \approx 1\text{GeV}$. $F(\tau)$ is a function of the scaling variable τ. In the framework of percolation of strings this result arises from the following parametrization of $\left(Q_s^A\right)^2$

$$\left(Q_s^A\right)^2 = \left(Q_s^p\right)^2 A^{\alpha(s)/2} N_A^{1/6}, \tag{3}$$

being N_A the number of wounded nucleons. $\alpha(s)$ and the proton saturation momentum are given, respectively, by the equations,

$$\alpha(s) = \frac{1}{3}\left(1 - \frac{1}{1 + \ln\left(\sqrt{s/s_0} + 1\right)}\right) \tag{4}$$

and

$$\left(Q_s^p\right)^2 = Q_0^2\left(\frac{W}{p_T}\right)^{\lambda}, \tag{5}$$

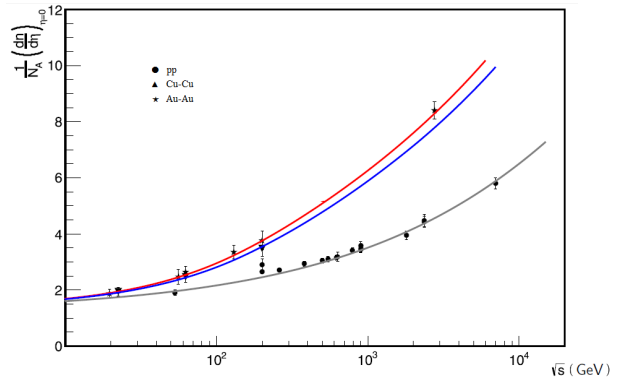

Figure 1. (Colour online.) Multiplicity dependence on $\sqrt{s}$. pp data from [31–37] (circles), CuCu (triangles) and AuAu (stars) from [38], PbPb (star) from [39]. Curves obtained from eq. (17): ($N_A = 1, A = 1$) for pp (grey line); ($N_A = 50, A = 63$) for CuCu (blue line); and ($N_A = 175, A = 200$) for AuAu/PbPb (red line). Color online.

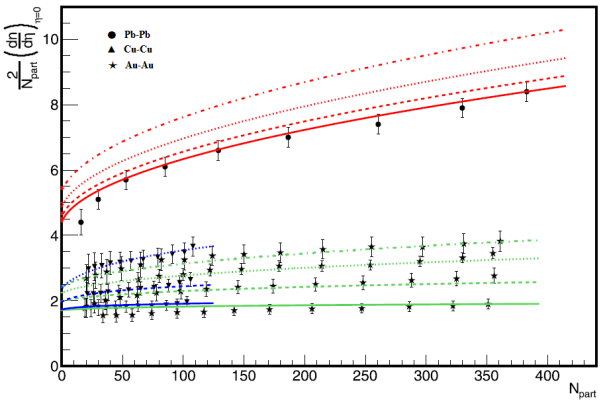

Figure 2. (Colour online.) Multiplicity dependence on centrality (the number of participating nucleons Npart = 2NA where NA is the number of participants per nucleus). CuCu (triangles) and AuAu (stars) data from [38], and PbPb (circles) from [39]. Curves: ($\sqrt{s}$ = 22.4, 62.4, 200 GeV) for CuCu (blue), ($\sqrt{s}$ = 19.6, 62.4, 130, 200 GeV) for AuAu (green), and ($\sqrt{s}$ = 2.76, 3.2, 3.9, 5.5 TeV) for PbPb (red). Color online.

with $Q_0 = 1$ GeV, $W = \sqrt{s} \times 10^{-3}$, $\sqrt{s_0} = 245$ GeV and $\lambda = 0.27$.

The function $\alpha(s)$ in (4) has to do with energy conservation in the multiparticle production process. In gluon saturation models, as in the glasma picture of the color glass condensate or in string percolation, color flux tubes (strings) are formed, which subsequently give rise to particles via fragmentation. Even at moderate high energies (RHIC energies) the number of color strings is very large for central heavy ion collisions. The fragmentation of strings requires a minimum of energy, around 0.5 GeV, to create at least a couple of hadrons. However, the total available energy is $A\sqrt{s}$ which, at low and intermadiate energies, is not enough to share with such a large number of strings. Asymptotically, the function $\alpha(s)$ goes to 1/3 and $\left(Q_s^A\right)^2$ for central collisions behaves, as usual, like $A^{1/3}$. This parametrization of $\alpha(s)$ has been previously used in the framework of percolation of strings to describe the multiplicity distributions of pp and AA collisions at all centralities and rapidities and at SPS, RHIC and LHC energies [28, 29]. The scale $\sqrt{s_0}$ indicates when the energy-momentum conservation effects become small and the behaviour of the effective number of collisions starts to change from N_A to $N_A^{4/3}$. The validity of this parametrization was tested in previous studies [30] and the results are shown in Fig. 1 and 2 in the form of fits to multiplicity distributions as a function of energy and centrality, respectively.

In Fig. 3, the overall geometrical scaling for all projectiles, targets and energies is shown. A reasonable scaling is observed in the range $0.2 < \tau < 1$. Detailed studies of the scaling have been previously done [23–26] showing different ratios of different type of collisions, specially for heavy ion collisions which are the main concern of our work.

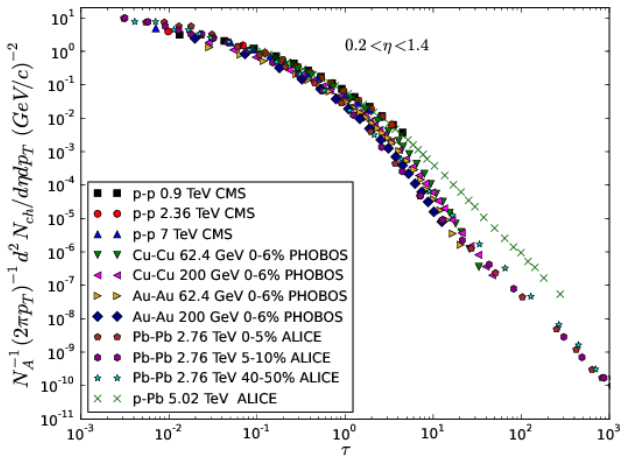

Figure 3. (Colour online.) Charged particle multiplicity per participant in the pseudorapidity range $0.2 < \eta < 1.4$ for all the heavy ion collisions considered [40–43] versus τ for $\lambda = 0.27$.

3 Geometrical scaling of the elliptic flow

In order to relate the geometrical scaling of the transverse momentum distribution, equation (1), with the scaling of the elliptic flow, we define an azimuthal angle saturation momentum, $Q_{s\varphi}^A$. As, on average, the gluon density is larger for smaller R_φ (smaller φ), we assume $\left(Q_{s\varphi}^A\right)^2 \sim 1/R_\varphi^2$. In addition, $Q_{s\varphi}^A$ should be proportional to the inverse of the mean free path, λ_{mfp}, normalized to the length size of the scattering, L, i.e. inversely proportional to the Knudsen number $k_n = \frac{\lambda_{mfp}}{L}$. Therefore, we can write:

$$\left(Q_{s\varphi}^A\right)^2 \equiv \frac{L}{\lambda_{mfp}} \frac{1}{R_\varphi^2} = \frac{1}{k_n R_\varphi^2} = \frac{Q_s^A L}{R_\varphi^2}. \qquad (6)$$

Notice that $\langle\left(Q_{s\varphi}^A\right)^2\rangle$ is not $\left(Q_s^A\right)^2$, indeed,

$$\langle\left(Q^A_{s\varphi}\right)^2\rangle = \frac{Q^A_s L}{\langle R^2_\varphi\rangle} = \frac{Q^A_s L}{R^2} \simeq \frac{\lambda_{mfp}\left(Q^A_s\right)^2}{L} \simeq k_n\left(Q^A_s\right)^2. \quad (7)$$

As $k_n = \frac{\lambda_{mfp}}{L}$ is very small for heavy nuclei collisions, $\langle\left(Q^A_{s\varphi}\right)^2\rangle << \left(Q^A_s\right)^2$.

Now, the scaling variable, $p_T^2 r_0^2 = p_T^2/\left(Q^A_s\right)^2$, should be replaced by

$$\tau_\varphi = p_T^2\left(r_0^2 + r_\varphi^2\right) = p_T^2\left(\frac{1}{(Q^A_s)^2} + \frac{1}{\left(Q^A_{s\varphi}\right)^2}\right). \quad (8)$$

As the integrated transverse momentum distributions decrease strongly with p_T, and $\langle\left(Q^A_{s\varphi}\right)^2\rangle$ is much smaller than $\left(Q^A_s\right)^2$, the contribution of the additional term to these distributions, concerning the geometrical scaling, is negligible. However, this term is responsible of the scaling of the elliptic flow. In fact,

$$v_2 = \frac{4\int_0^{\pi/2} d\varphi \cos 2\varphi \frac{dN}{dp_T^2 d\varphi}}{\frac{dN}{dp_T^2}} = \frac{4\int_0^{\pi/2} d\varphi \cos 2\varphi F(\tau_\varphi)}{F(\tau)}. \quad (9)$$

Expanding $F(\tau_\varphi)$ in powers of $R^2_\varphi - R^2$ and retaining the first non-vanishing term, we have,

$$v_2 = \frac{2}{\pi}\int_0^{\pi/2} d\varphi \cos 2\varphi \frac{R^2 - R^2_\varphi}{R^2}\frac{4}{F(\tau)}\frac{dF}{d\tau}\tau Q^A_s L, \quad (10)$$

where we approximate $L \approx R$.

Denoting by

$$\frac{4}{F(\tau)}\frac{dF}{d\tau} = \varphi(\tau), \quad (11)$$

we have

$$v_2 = \epsilon_1 Q^A_s L \tau\varphi(\tau) \quad (12)$$

or

$$v_2 k_n = \epsilon_1 \tau\varphi(\tau), \quad (13)$$

which is the scaling law we were looking for, where

$$\epsilon_1 = \frac{2}{\pi}\int_0^{\pi/2} d\varphi \cos 2\varphi \frac{R^2 - R^2_\varphi}{R^2}, \quad R_\varphi = \frac{R_A \sin(\varphi - \alpha)}{\sin\varphi}, \quad (14)$$

and

$$\alpha = \arcsin(\frac{b}{2R_A}\sin\varphi), \quad R^2 = \langle R^2_\varphi\rangle = \frac{2}{\pi}\int_0^{\pi/2} d\varphi R^2_\varphi \quad (15)$$

being R_A the radius of the nucleus and L the length associated to the size of the collision area at a given impact parameter and energy. Indeed, the product $Q^A_s L$ is the inverse of the Knudsen number, k_n, i.e., the mean free path normalized to the length measured as the number of scattering centers.

ϵ_1 is a measure of the eccentricity of the collision. It does not depend on the distribution of scattering centers (partons or nucleons) in the transverse plane and it is determined only by the almond shape of the collision at a given impact parameter.

The scaling law obtained for v_2 is based exclusively on two ingredients: the geometrical scaling of transverse momentum distributions for $\tau < 1$ (intial state effect) and the assumption for the azimuthal saturation momentum (6) which encodes all the angle dependence. The main question is whether the assumption (6) can be considered as a natural consequence of the structure of the initial state or, on the contrary, it is a final state effect. On the one hand, the possibility of domains of color flux tubes or clusters of strings having different azimuthal angles, has been pointed out in several approaches [15–17, 20]. This would be the origin of the ridge structure. In this inital state approach the equation (6) is a natural assumption. On the other hand, the mean free path or the Knudsen number of equation (6) can be regarded as a measure of the path needed to way out the collision and, consequently, as a measure of the energy lost by the partons produced in the fragmentation of a color flux tube (or in a cluster of strings) interacting with the color field of other color flux tubes [21].

4 Comparison with experimental results

In Fig. 4 (a) we plot the measured values of $v_2(p_T)$ for Au-Au collisions for different centralities at RHIC [44] and for PbPb collisions at LHC [45] divided by the product $\epsilon_1 Q^A_s L$ computed for each centrality and energy. We take the usual values of b and N_A for each centrality to compute ϵ_1 and Q^A_s using the equations (14), (15) and (3) respectively. L is a measure of the number of longitudinal scatterings, which in the Glauber model is proportional to $N_A^{1/3}$. Nevertheless, we use $(1 + N_A^{1/3})/2$, which is used by most of the strings models as dual parton model [46, 47], quark gluon string model [48], Venus [49] or EPOS [50]. The solid black line corresponds to a fit to these data, given by

$$\frac{v_2}{\epsilon_1 Q^A_s L} = a\tau^b, \quad (16)$$

where $a = 0.1264 \pm 0.0076$ and $b = 0.404 \pm 0.025$.

The Fig. 4 shows that this scaling is satisfied.

In order to see the quality of this scaling we show in Fig. 4 (b) the ratio of Pb-Pb 10-20 % at 2.76 TeV, Pb-Pb 40-50 % at 2.76 TeV, Au-Au 20-30% at 200 GeV and Au-Au 30-40% at 200 GeV over Pb-Pb 30-40% at 2.76 TeV as a function of τ. All the ratios lie in the range $0.8 - 1.15$ for the whole τ considered, showing that the scaling is quite good (most of the experimental error data are of the order of 10%).

Changing the eccenticity, ϵ_1, by the usual eccentricity, $\epsilon = \langle y^2 - x^2\rangle/\langle y^2 + x^2\rangle$, or by the participant eccentricity, the scaling is not satisfied for both Monte-Carlo Glauber and Color Glass distributions.

Assuming that the v_2 scaling can be extended to pp collisions, we compute the elliptic flow as a function of the trasnsverse momentum, $v_2(p_T)$, for $\tau < 1$. In Fig. 5 we

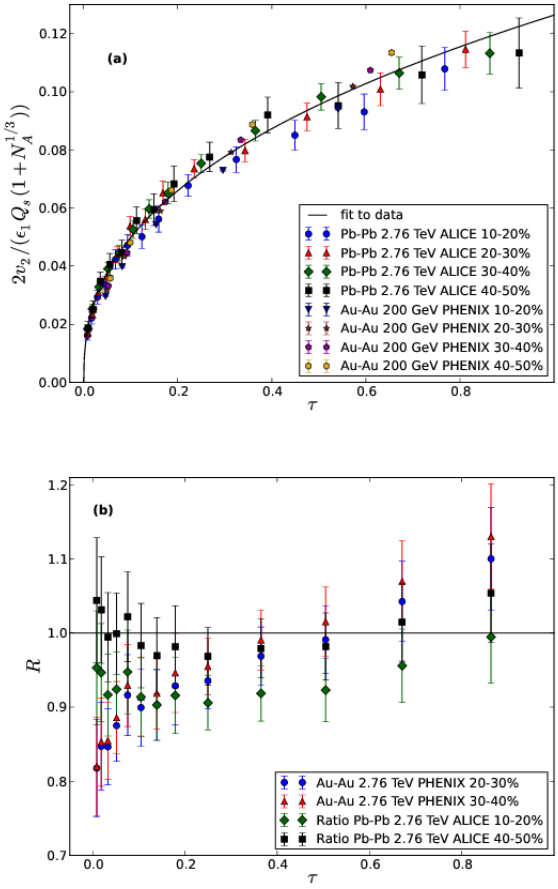

Figure 4. (Color online.) **(a)** v_2 divided by the product $\epsilon_1 Q_s^A L$ for 10-20%, 20-30%, 30-40% and 40-50% Au-Au collisions at 200 GeV [44], for 10-20%, 20-30%, 30-40% and 40-50% Pb-Pb collisions at 2.76 GeV [45] in terms of τ. The solid black line is a fit to data according to (16). **(b)** Ratio of Pb-Pb 10-20%, Pb-Pb 40-50% at 2.76 TeV [45], Au-Au 20-30% and Au-Au 30-40% at 200 GeV [44] over Pb-Pb 30-40% at 2.76 TeV [45] versus τ.

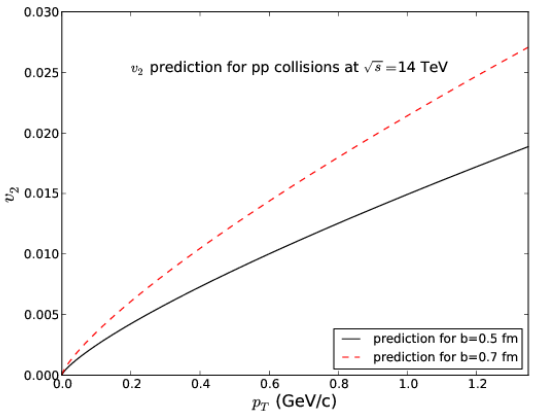

Figure 5. (Color online.) v_2 prediction for pp collisions at $\sqrt{s}$ = 14 TeV for impact parameters values of b = 0.5 fm (solid black curve) and b = 0.7 fm (dashed red curve) as a function of p_T.

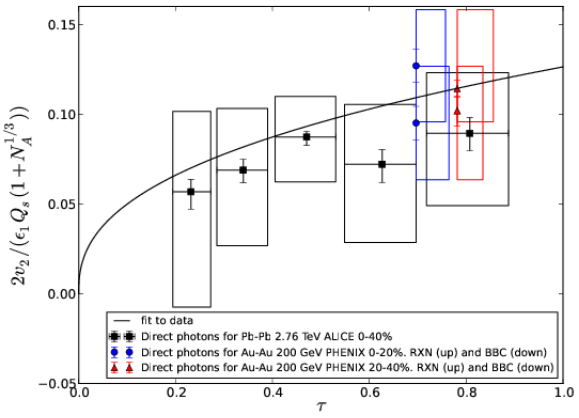

Figure 6. (Color online.) v_2 divided by the product $\epsilon_1 Q_s^A L$ for direct photons at 0-20% and 20-40% Au-Au collisions at 200 GeV [54] and direct photons at 0-40% Pb-Pb collisions at 2.76 GeV [55] plotted as a function of τ. The solid black line is a fit to data according to (16).

show our predictions for $\sqrt{s}$ = 14 TeV and for impact parameters values of b = 0.5 fm and b = 0.7 fm.The $v_2(p_T)$ obtained is much smaller than the computed one using hot spots inside the proton [51] and only slightly smaller than the one found considering usual impact parameter distributions [52, 53]. For b = 0.7 the multiplicity would not be very different from the minimum bias which in many models is predicted to be around 7.2 at central rapidity [28].

We have not included in our analysis the v_2 data on pPb collisions due to the uncertainties in the values of N_A at a given impact parameter. Moreover, in this stage of our research, we have not studied the scaling for specified particles. As far as geometrical scaling is satisfied for π, κ and p [25], we expect that there will also be a v_2 scaling for identified particles, using $m_T - m$ instead of p_T. In this way, we could compute $v_2(p_T)$ of any particle whose momentum distribution verifies the scaling.

In addition, since direct photon production satisfies geometrical scaling [27], its elliptic flow may be of the same size and p_T shape of the rest of particles. In order to check this point, in Fig. 6 we plot the ALICE preliminary data [55] and the PHENIX data [54] at different centralities. PHENIX collaboration quote two different points at the same p_T and centrality obtained by different analysis methods (BBC and RXN detectors). In any case, we observe that the data are close to the scaling curve.

5 Conclusions

We have shown that the experimental data on the eliptic flow of charged particles for Au-Au and Pb-Pb collisions for different centralities at RHIC and LHC energies satisfy a scaling law. The photon data, despite their large uncertainties, also satisfy this scaling. Other than the eccentricity, this scaling law involves the number of scatterings and a function which depends only on $p_T^2/\left(Q_s^A\right)^2$. The number

of scatterings in the only involved quantity in relation with final state effects. The rest has to do with the geometry and gluon saturation.

The scaling law obtained can be related to the known geometrical scaling of the transverse momentum distributions by encoding the azimuthal dependence is a new saturation momentum which, besides this angular dependece, is proportional to the number of scatterings. This saturation momentum can be interpreted as the lost of momentum of a parton in its way out of the collision.

It would be interesting to look for a scaling law similiar to (13) for the rest of the harmonic moments. The total distribution might factorize in two terms: one with the product of the number of scatterings and a scaling function on $p_T^2/\left(Q_s^A\right)^2$ and the other with the sum of the products of the different eccentricities with the corresponding azimuthal dependence.

Acknowledgements

We thank N. Armesto for very useful discussions. This work has been done under the project FPA2011-22776 of MINECO (Spain), the Spanish Consolider CPAN project, FEDER funds and Xunta de Galicia.

References

[1] K. Adrox *et al.* (PHENIX Collaboration), Nucl. Phys. **A757**, 184 (2005)
[2] J. Adams *et al.* (STAR Collaboration), Nucl. Phys. **A757**, 102 (2005)
[3] A.K. Aamodt *et al.* (ALICE Collaboration), Phys. Rev. Lett. **105**, 252302 (2010)
[4] J. Adams *et al.* (STAR Collaboration), Phys. Rev. **C73**, 064907 (2006)
[5] A. Adare *et al.* (PHENIX Collaboration), Phys. Rev. **C78**, 014901 (2008)
[6] B. Alver *et al.* (PHOBOS Collaboration), Phys. Rev. **C81**, 034915 (2010)
[7] S. Chatrchyan *et al.* (CMS Collaboration), Eur. Phys. J. **C72**, 10052 (2012)
[8] B. Abelev *et al.* (ALICE Collaboration), Phys. Lett. **B719**, 29 (2013)
[9] S. Chatrchyan *et al.* (CMS Collaboration), Phys. Lett. **B718**, 795 (2013)
[10] V. Khachatryan *et al.* (CMS Collaboration), JHEP **1009**, 091 (2010)
[11] S. Gavin, L. McLerran, G. Moschelli, Phys. Rev. **C79**, 051902 (2009)
[12] K. Dusling, R. Venugopalan, Phys. Rev. **D87**, 054014 (2013)
[13] A. Bzdak, B. Schenke, P. Tribedy, R. Venugopalan, Phys. Rev. **C87**, 064906 (2013)
[14] A. Dumitru et al., Phys. Lett. **B697**, 21 (2011)
[15] A. Kovner, M. Lublinsky, Phys. Rev. **D83**, 034017 (2011)
[16] A. Kovner, M. Lublisnky, Int. J. of Mod. Phys. **E22**, 1330001 (2013)
[17] A. Dumitru, A. Giannini, arXiv:1406.5781 [hep-ph] (2014)
[18] Y.V. Kovchegov, D.E. Wertepny, Nucl. Phys. **A906**, 50 (2013)
[19] K. Werner, I. Karpenko, T. Pierog, Phys. Rev. Lett. **106**, 122004 (2011)
[20] I. Bautista, J. Dias de Deus, C. Pajares, Eur. Phys. J. **C72**, 2038 (2012)
[21] M.A. Braun, C. Pajares, V. Vechernin, Nuc. Phys. **A906**, 14 (2013)
[22] G. Torrieri, Phys. Rev. **C89**, 024908 (2014)
[23] L. McLerran, M. Praszalowicz, Acta Phys. Polon. **B41**, 1917 (2010)
[24] M. Praszalowicz, Phys. Rev. Lett. **106**, 142002 (2011)
[25] M. Praszalowicz, Phys. Lett. **B727**, 461 (2013)
[26] C. Andrés, A. Moscoso, C. Pajares, Nucl. Phys. **A901**, 14 (2013)
[27] C. Klein-Boesingand, L. McLerran, arXiv:1403.1174v1 [nucl-th] (2013)
[28] I. Bautista, J.G. Milhano, C. Pajares, J. Dias de Deus, Phys. Lett. **B715**, 230 (2012)
[29] I. Bautista, C. Pajares, J.G. Milhano, J. Dias de Deus, Phys. Rev. **C86**, 034909 (2012)
[30] I. Bautista, J. Dias de Deus, J. Guilherme Milhano, C. Pajares, Phys. Lett. B **715**, 230 (2012)
[31] UA1 Collaboration, Nucl. Phys. B **335**, 261 (1990)
[32] G. J. Alner *et al.* (UA5 Collaboration), Phys. Rep. **154**, 247 (1987)
[33] STAR Collaboration, Phys. Rev. C **79**, 034909 (2009)
[34] CDF Collaboration, Phys. Rev. D **41**, 2330 (1990)
[35] K. Aamodt *et al.* (ALICE Collaboration), Eur. Phys. J. C **68**, 89 (2010)
[36] V. Khachatryan *et al.* (CMS Collaboration), JHEP **1002**, 041 (2010)
[37] V. Khachatryan *et al.* (CMS Collaboration), Phys. Rev. Lett. **105**, 022002 (2010)
[38] B. Alver *et al.* (PHOBOS Collaboration), Phys. Rev. C **83**, 024913 (2011)
[39] K. Aamodt *et al.* (ALICE Collaboration), Phys. Rev. Lett. **106**, 032301 (2011)
[40] B.B. Back *et al.* (PHOBOS Collaboration), Phys. Rev. Lett. **94**, 082304 (2005)
[41] B. Alver *et al.* (PHOBOS Collaboration), Phys. Rev. Lett. **96**, 212301 (2006)
[42] B. Abelev *et al.* (ALICE Collaboration), Phys. Lett. **B720**, 52 (2013)
[43] B. Abelev *et al.* (ALICE Collaboration), Phys. Rev. Lett. **110**, 082302 (2013)
[44] A. Adare *et al.* (PHENIX Collaboration), Phys. Rev. Lett. **98**, 162301 (2007)
[45] A. Aamodt *et al.* (ALICE Collaboration), Phys. Rev. Lett. **105**, 252302 (2010)
[46] A. Capella et al., Phys. Rep. **236**, 225 (1994)
[47] A. Capella, C. Pajares, A.V. Ramallo, Nucl. Phys. **B241**, 75 (1984)

[48] A.B. Kaidalov, K.A. Ter-Martirosyan, Phys. Lett. **B117**, 247 (1982)
[49] K. Werner, Phys. Rep. **232**, 87 (1992)
[50] K. Werner et al., Nucl. Phys. Proc. Suppl. **B196**, 36 (2009)
[51] J. Casalderrey-Solana, U.A. Wiedemann, Phys. Rev. Lett. **104**, 102301 (2010)
[52] D. d'Enterria et al., Eur. Phys. J. **C66**, 173 (2010)
[53] L. Cunqueiro et al., Eur. Phys. J. **C65**, 423 (2010)
[54] A. Adare *et al.* (PHENIX Collaboration), Phys. Rev. Lett. **109**, 122302 (2012)
[55] D. Lohner (for the ALICE Collaboration), J. Phys. Conf. Ser. **446**, 012028 (2013)